# Genomic glucocorticoid signaling in the hippocampus: understanding receptor specificity and context dependency

Weert, L.T.C.M. van

# CHAPTER 2

# NeuroD factors discriminate mineralocorticoid from glucocorticoid receptor DNA binding in the male rat brain

Lisa T.C.M. van Weert[1,5,6], Jacobus C. Buurstede[1], Ahmed Mahfouz[2,3], Pamela S.M. Braakhuis[1], J. Annelies E. Polman[4], Hetty C.M. Sips[1], Benno Roozendaal[5,6], Judit Balog[7], E. Ronald de Kloet[1,4], Nicole A. Datson[4], Onno C. Meijer[1]

Endocrinology 2017, 158(5):1511-1522

[1] Department of Medicine, Division of Endocrinology, Leiden University Medical Center, Leiden, The Netherlands
[2] Department of Radiology, Division of Image Processing, Leiden University Medical Center, Leiden The Netherlands
[3] Delft Bioinformatics Lab, Delft University of Technology, Delft, The Netherlands
[4] Division of Medical Pharmacology, Leiden/Amsterdam Center for Drug Research, Leiden, The Netherlands
[5] Department of Cognitive Neuroscience, Radboud University Medical Center, Nijmegen, The Netherlands
[6] Donders Institute for Brain, Cognition and Behaviour, Radboud University, Nijmegen, The Netherlands
[7] Department of Human Genetics, Leiden University Medical Center, Leiden, The Netherlands

# Abstract

In the limbic brain, mineralocorticoid receptors (MRs) and glucocorticoid receptors (GRs) both function as receptors for the naturally occurring glucocorticoids (corticosterone/cortisol), but mediate distinct effects on cellular physiology via transcriptional mechanisms. The transcriptional basis for specificity of these MR- versus GR-mediated effects is unknown. To address this conundrum we have identified the extent of MR/GR DNA binding selectivity in the rat hippocampus using chromatin immunoprecipitation followed by sequencing (ChIP-seq). We found 918 and 1450 non-overlapping bindings sites for MR and GR, respectively. Furthermore, 475 loci were co-occupied by MR and GR. *De novo* motif analysis resulted in a similar binding motif for both receptors at 100% of the target loci, which matched the known glucocorticoid response element (GRE). In addition, the Atoh/NeuroD consensus sequence was found in co-occurrence with all MR-specific binding sites, but was absent for GR-specific or MR-GR overlapping sites. bHLH family members Neurod1, Neurod2 and Neurod6 showed hippocampal expression and were hypothesized to bind the Atoh motif. Neurod2 was detected at rat hippocampal MR binding sites, but not at GR-exclusive sites. All three NeuroD transcription factors acted as DNA-binding dependent coactivators for both MR and GR in reporter assays in heterologous HEK293 cells, likely via indirect interactions with the receptors. In conclusion, a NeuroD family member binding to an additional motif near the GRE seems to drive specificity for MR over GR binding at hippocampal binding sites.

# Introduction

The endogenous glucocorticoid hormone of the rat, corticosterone, has a profound action on the brain. This action is mediated in a complementary manner by mineralocorticoid receptors (MRs) and glucocorticoid receptors (GRs), which are unevenly distributed over the brain, but co-expressed in abundance in the hippocampus (1). The high affinity MRs are already substantially occupied with low corticosterone levels (2). In the initial response to stress, these MRs play a crucial role in retrieval of stressful information and the selection of an appropriate coping response (3-5). In contrast, the lower affinity GRs become activated only at higher corticosterone levels, around the peak of the circadian rhythm and during a stress response. GR activation promotes memory storage of the stressful experience (6, 7) and behavioral adaptation and recovery (1, 8).



Much progress has been made in understanding the cellular mechanism of these coordinated MR-GR mediated actions of corticosterone (9). Many of the effects depend on the transcriptional activity of the receptors. MR-mediated actions generally raise excitability in the hippocampus. In the most ventral part of the hippocampus corticosterone prolongs excitability via GR, providing an extended period for encoding of new information. In the dorsal pyramidal cells GR-mediated actions oppose those mediated by MR (10). That these MR- and GR-mediated effects of corticosterone are sometimes overlapping and in other processes are distinct is remarkable, given the large structural similarity between the two receptor types.

MR and GR are members of the nuclear receptor family, with a modular structure of an N-terminal domain (NTD), a DNA binding domain (DBD) and C-terminal ligand binding domain (LBD). Upon ligand binding, the receptors can dimerize and translocate to the nucleus, where they alter the transcription of their target genes. MR and GR can affect gene expression via tethering to other proteins such as AP-1 and NFκB (11), but in the hippocampus, at least under basal conditions, the main mechanism seems to be via direct DNA binding to the glucocorticoid response element (GRE) – palindromic sequences that are variations of AGAACANNNTGTTCT (12). Homo- as well as heterodimers of the receptors may occur (13, 14). The intrinsically unstructured NTD contains an Activator Function (AF)-1, and the LBD contains a ligand-dependent AF-2. Through these AF domains the receptors can interact with coregulators, which can modulate the transcriptional effects by histone modifying activity and recruitment/stabilization of the transcription factor complex (15). The fact that the two receptors are 94% identical in their DBD (16), suggests

that other mechanisms must exist that confer transcriptional specificity underlying the differential effects of MR/GR.

It has remained elusive to what extent genomic targets of MR and GR overlap and what determines the specificity of MR and GR DNA binding. We previously identified genomic loci for GR, using chromatin immunoprecipitation-sequencing (ChIP-seq) after a single injection of corticosterone (12). In the current study we aimed to characterize mechanisms that confer MR/GR specificity by directly comparing their genomic binding sites in the same tissue. Our findings suggest that interactions between MR/GR and DNA-binding transcription factors from the NeuroD family are responsible for MR-selective signaling in the limbic brain, and that NeuroD factors are able to potentiate transcriptional activity of both receptor types *in vitro*.

# Material and methods

## In vivo experiment

For the ChIP-seq experiment, adult male Sprague Dawley rats (Harlan, The Netherlands) were housed on a 12:12-hour light/dark cycle (lights on 7:30 AM) with food and water *ad libitum*. ChIP-seq with MR, GR or control immunoglobulin G (IgG) antibody was performed on hippocampal tissue of 3 day adrenalectomized animals 60 min after a single intraperitoneal injection of 300 or 3000 μg/kg corticosterone as a 2-hydroxypropyl-β-cyclodextrin complex (CORT-HBC), as described (12). ChIP-seq was done on pooled tissue from 6 animals per treatment, which was redivided leading to 4 technical ChIP replicates for both MR and GR. All experiments were performed according to the European Commission Council Directive 2010/63/EU and the Dutch law on animal experiments and approved by the animal ethical committee from Leiden University.

## ChIP-sequencing analysis and motif search

The MR binding data were generated and analyzed in parallel with the previously published data for GR (12). Illumina Genome Analyzer 35 bp single end reads were uniquely mapped to the rattus norvegicus genome version 4 (rn4). Peaks were called using Model-based Analysis of ChIP-Seq (MACS) (17) with the IgG antibody binding dataset as the background. Binding sites were considered overlapping if more than 4 bp were shared. Data were visualized by uploading wiggle files to Integrative Genomics Viewer (IGV) (18). Using the annotate peak function of HOMER, binding sites were associated

to their nearest gene (19). The Database for Annotation, Visualization and Integrated Discovery (DAVID) was used for gene ontology analysis (20). Binding sequences were analyzed for the presence of *de novo* motifs using Multiple Expectation maximization for Motif Elicitation (MEME) (21). The motif size was set from 6 bp min to 20 bp max, searching also the reverse complement, with a maximum of 10 output motifs, using random shuffled input sequences as background model. Enriched motifs were compared against the JASPAR vertebrate database of known motifs using TOMTOM motif comparison tool. Analysis of Motif Enrichment (AME) was used for enrichment analysis of known motifs in MR-exclusive relative to GR-exclusive binding sequences, and Motif Alignment & Search Tool (MAST) for directed search of motifs of interest, under default settings (21).



## ChIP-qPCR validation

For binding site validation we performed ChIP-qPCR on hippocampal tissue of adrenally intact rats sacrificed at the time of their endogenous corticosterone peak. Antibodies used are listed in **Supplemental Table 1**. Protease inhibitors (Roche) were added to all buffers during tissue processing and the ChIP procedure. Hippocampal hemispheres were fixated with 1% formaldehyde for 12-14 min and were homogenized in Jiang buffer (0.32 M sucrose, 5 mM CaCl2, 3 mM Mg(Ac)2, 0.1 mM EDTA, 10 mM Tris-HCl pH 8.0, 0.1% Nonidet P (NP)-40) using a glass douncer (Kimble-Chase). Following steps were performed in NP buffer (150 mM NaCl, 50mM Tris-HCl pH 7.5, 5 mM EDTA, 0.5% NP-40, 1% Triton X-100). Chromatin was fragmented by sonication for 32 min, 30 sec ON/30 sec OFF cycles, using a Bioruptor Pico (Diagenode). Three processed hippocampal hemispheres were pooled and redivided to perform a ChIP for both MR and Neurod2. From each chromatin sample an aliquot was taken as input material, to be able to calculate the percentage of immunoprecipitated DNA. Chromatin (500 µL) was incubated overnight with 6 µg antibody, after which 20 µL protein A Sepharose beads (GE healthcare) were added for 2.5 hours. After several washing steps (**Supplemental Methods**), antibody-bound DNA was eluted from the beads using 10% Chelex 100 (Bio-Rad), further purified by phenolization and dissolved in 50 µL $H_2O$. qPCR was performed on 4x diluted ChIP samples according to the protocol described below. Primers were designed to span the GRE of the discovered binding sites, and are listed in **Supplemental Table 2**.

## Reporter assays

For mechanistic insights into the effect of NeuroD factors on MR/GR promoter activity, we performed luciferase reporter assays. HEK293 cells (human embryonic kidney, female)

were cultured in Dulbecco's Modified Eagle Medium with GlutaMax (Gibco) containing 100 U/mL penicillin and 100 µg/mL streptomycin (Gibco) and 10% fetal bovine serum (FBS, PAN-Biotech), at 37°C under 5% $CO_2$. For the reporter assays, cells were seeded in a 24-wells plate at a density of 80,000 cells/well and grown in medium supplemented with charcoal stripped FBS (Sigma) to exclude cortisol action from the serum. Cells were transfected on day 2 with luciferase construct (TAT1-Luc or TAT3-Luc: 25 ng/well; GRE-At, MRE-At or GRE-MutAt: 30 ng/well), expression vector for one of the receptors (MMM, ∆MM, MM∆, GGG, ∆GG, GG∆: 10 ng/well), pCMV-Myc-Neurod1/2/6 (0-1-3-10-50-100 ng/well), completed with pcDNA3.1 to a total of 300 ng/well and 1.25 µL/well FuGENE (Promega) in unsupplemented DMEM. Renilla luciferase was used to correct for transfection efficiency (1 ng/well, pRL-CMV, Promega). On day 3, cells were stimulated with corticosterone ($10^{-7}$ M or at indicated concentrations, Sigma) dissolved in ethanol, diluted in medium with a final concentration of 0.1 % ethanol. After 24 hours the cells were washed with phosphate buffered saline and reporter protein was measured using the Dual-luciferase Reporter Assay System according to the manufacturer's instruction (Promega). Briefly, 100 µL lysis buffer was added and after 10 min 10 µL lysate was transferred into a half area 96-wells plate. Luciferase levels were quantified with 25 µL luciferase assay substrate at 570 nm; subsequently Renilla signal was measured at 470 nm after the addition of 25 µL Stop & Glo at a SpectraMax L microplate reader (Molecular Devices). All data are presented as mean ± SEM. Reporter assays were done in triplicates, and repeated at least once.

## Plasmids

The GRE-At and GRE-MutAt luciferase constructs were created by inserting a 36-bp fragment containing a perfect palindromic GRE plus the Atoh1 motif or the GRE with a scrambled motif in the XhoI site of a pGL4.10[luc2] vector (Promega). Inserts were GRE-At: ctcgagGATGGCAGATGGAGCTAAGAACAGAATGTTCTATAActcgag and GRE-MutAt: ctcgagGATGGAGCGGATAGCTAAGAACAGAATGTTCTATAActcgag. The MRE-At luciferase construct was created by inserting a 35-bp endogenously found MR binding site containing a more degenerate GRE plus the Atoh1 motif in the NheI/BglII site of the same pGL4 vector. MRE-At insert was: gctagcGCACACAGATGAGTGGGGATCTGAATGTACTGTGGagatct. The pCMV-Myc-Neurod6 expression vector was kindly provided by Dr. Mitsuhiko Yamada (22). *Neurod1* and *Neurod2* were amplified from Sprague Dawley rat hippocampal cDNA using the primers forward 5'-CAGTAGTCGACCATGACCAAATCATACAGCGAG-3', reverse 5'-GTACTCTCGAGTGCCTCTAATCGTGAAAGATGG-3' and forward 5'-CAGTAGTCGACCATGCTGACCCGCCTGTT-3', reverse

5'-GTACTCTCGAGAGGTCTCAGTTATGGAAAAACGC-3' respectively and cloned in frame into the SalI/XhoI site of the same pCMV-Myc vector to gain pCMV-Myc-Neurod1 and pCMV-Myc-Neurod2. Expression vectors for rat receptors 6RMR (MMM), 6RGR (GGG) and their corresponding truncated receptors 6RMR/596C (ΔMM), 6RMR/N689 (MMΔ), 6RGR/407C (ΔGG), 6RGR/N525 (GGΔ), and TAT1/3-Luc reporters were kindly provided by Dr. David Pearce (23).

## Real-time quantitative PCR

To validate the NeuroD factor expression in the rat brain, we performed RT-qPCR measurements on Sprague Dawley tissue. Hippocampal hemispheres were homogenized in TriPure (Roche) by shaking the tissue with 1.0 mm diameter glass beads for 20 s at 6.5 m/s in a FastPrep-24 5G instrument (MP Biomedicals). Total RNA was isolated with chloroform, precipitated with isopropanol, washed with 75% ethanol and resuspended in nuclease-free $H_2O$. The purity and concentration of the RNA samples were measured on a NanoDrop 1000 spectrophotometer (Thermo Scientific). cDNA was reverse transcribed from 1 µg RNA using random hexamers and M-MLV reverse transcriptase (Promega), incubated for 10 min at 25°C, 50 min at 45°C and 10 min at 70°C. RT-qPCR was performed in duplo on 10x diluted cDNA (5 ng/µL) with final primer concentrations of 0.5 µM using GoTaq qPCR master mix (Promega) in a CFX96 real-time PCR machine (Bio-Rad). The program consisted of 40 cycles of 10 s at 95°C and 30 s at 60°C, followed by a melting curve generation from 65°C to 95°C in steps of 0.5°C. Primer sequences are listed in **Supplemental Table 2**.

## Allen Brain Atlas correlations

Lists of MR-exclusive, MR-GR overlapping and GR-exclusive genes corresponding to the intragenic and distal promoter (up to -5000 bp) ChIP-seq binding sites were evaluated for their co-expression with each studied NeuroD factor, using the mouse brain gene expression data from the Allen Brain Atlas (24). Pearson's correlation coefficient was used as a measure of similarity between the expression profile of the seed genes (*Neurod1*, *Neurod2* and *Neurod6*) and every gene in the three aforementioned lists within an anatomical region of interest (25). Correlations were calculated in the hippocampus, and its subregions cornu ammonis (CA)1 to CA3 and the dentate gyrus (DG) as well as the striatum. In order to assess the strength of the association between each gene list and a seed gene, we used a one-sided Wilcoxon rank-sum test.

## Data deposition

ChIP-seq data have been submitted to the European Nucleotide Archive (ENA) and are publicly available under accession number PRJEB18916.

# Results

## MR-GR binding site overlap

ChIP-seq on hippocampus chromatin with MR and GR antibodies resulted in the generation of 1.3-1.9x$10^7$ reads per sample. After uniquely mapping 66.6-83.5% of these reads to the rat genome (rn4), MACS peak calling with a false discovery rate (FDR) cut-off at 13.5% (conform Polman et al., 2013; **Supplemental Figure 1A**) resulted in 768 MR sites in the animals injected with 300 µg/kg (MR300), and 1465 MR sites and 2460 GR sites in the animals injected with 3000 µg/kg (MR3000 and GR3000).

We computed the overlap in binding site genomic coordinates for MR and GR (**Figure 1A**). Additional filtering of MR- and GR-exclusive sites demanded total absence of any peak (the MACS lists including those peaks with an FDR above 13.5%) at the same locus in the GR and MR data, respectively. This resulted in 918 MR-exclusive sites (combined from the MR300 and MR3000 dataset), 475 MR-GR overlapping sites and 1450 GR-exclusive sites (**Supplemental Table 3**). These correspond to 45.9% of the total MR sites and 58.9% of the total GR sites being non-overlapping. ChIP-seq traces of an MR-exclusive, MR-GR overlapping and GR-exclusive peak are shown in **Supplemental Figure 2**. The distribution of sites relative to nearest genes is similar for these subsets, with approximately 40-45% of the binding sites located within promoters and genes - mainly in introns (**Supplemental Figure 1B**). Limited overlap was found between the MR binding sites for the two different dosages, as only 30.6% of the MR300 sites were also found in the MR3000 dataset.

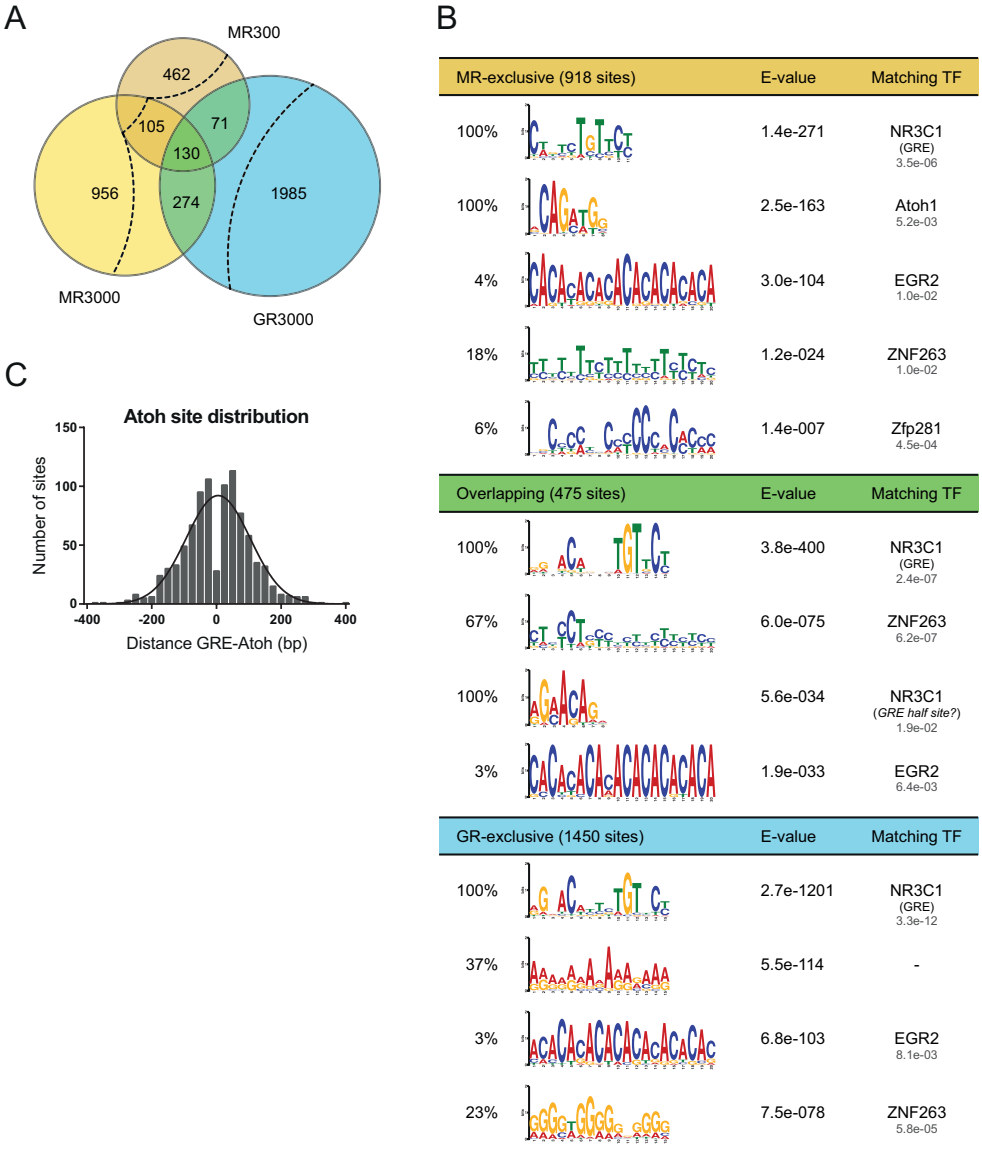


**Figure 1**. ChIP-seq binding site analysis. **A)** Overlap of MR and GR binding sites in the rat hippocampus, from animals injected with 300 µg/kg (MR300) or 3000 µg/kg (MR3000 and GR3000) corticosterone. Dashed lines represent the additional filtering of non-overlapping sites demanding total absence of any peaks in the other receptor dataset, leading to 918 MR-exclusive (combined from MR300 & MR3000), 475 overlapping and 1450 GR-exclusive sites. **B)** *De novo* motif analysis of MR-exclusive, overlapping and GR-exclusive binding sites. Discovered motifs are depicted with their E-value (MEME) and the highest ranked matching transcription factor (TF). Listed TFs are followed by the E-value (TOMTOM) for the motif comparison. **C)** Distribution of distance between GRE and Atoh motifs over 25 bp bins, including a normal curve. Depletion of the histogram bin around zero is due to the minimum distance of 8bp as calculated from the center of the GRE to the center of the Atoh motif.

## Validation of MR binding sites

The GR binding sites were thoroughly validated before (12). We performed ChIP-qPCR measurements for MR in the hippocampus of adrenally intact animals sacrificed at the time of their endogenous corticosterone peak. MR binding was detected at all tested MR-exclusive sites, whereas no MR signal was found at any of the GR-exclusive sites (**Figure 2A**). This demonstrates that the selectivity found in the pharmacological ChIP-seq experiment, also occurs in a physiological context.

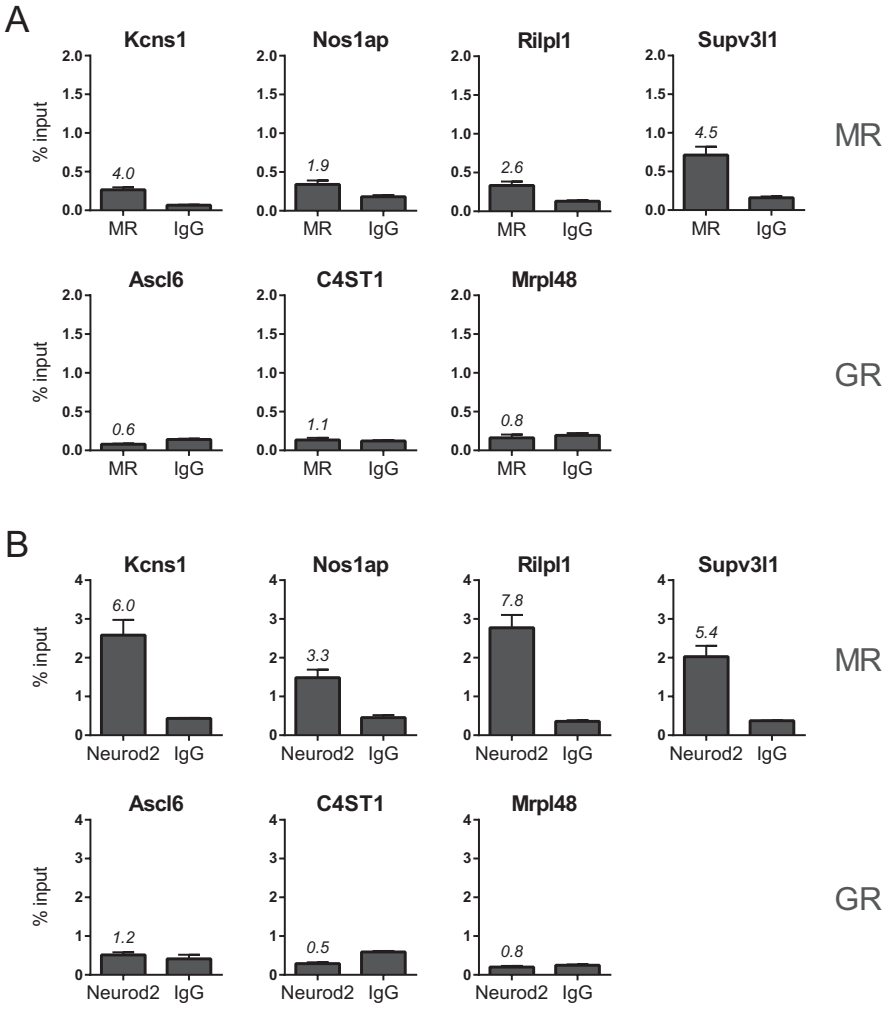


**Figure 2**. ChIP-qPCR validation of **A)** MR (n=5) and **B)** Neurod2 (n=6) binding to a subset of MR-exclusive and GR-exclusive binding sites. Numbers indicate the fold induction over IgG background.

## Processes associated with MR and GR target genes

The biological relevance of the hippocampal binding sites was examined by gene ontology enrichment analysis of target genes, under the assumption that expression of MR/GR bound genes will be regulated by the receptor. Intragenic and upstream (up to -5kb) binding sites were annotated to generate lists of MR-exclusive, overlapping and GR-exclusive target genes (**Supplemental Table 4**). Functional annotation clustering using DAVID showed enrichment of brain-related terms, such as *Regulation of cell projection assembly* (MR), *Synapse, Regulation of synaptic plasticity* (overlapping) and *Cell/neuron projection, Synaptic vesicle* (GR) (**Supplemental Table 5**). Interestingly, for those genes linked to specific MR binding there was enrichment for *Sodium channel activity*, *Calcium ion transport* and *Ion transport, voltage-gated channel activity*. Another term specific for MR-exclusive target genes was *Cell adhesion*. Furthermore the annotated GR-exclusive target genes were associated with *Apoptosis* and *Response to oxidative stress*.



## An additional motif was found near MR-exclusive sites

To explore the biological mechanism underlying MR/GR-selective binding, we performed *de novo* motif analysis on the binding site sequences. For the MR, as well as the overlapping and GR datasets, all sites contained a glucocorticoid response element (GRE) (**Figure 1B**). This is in contrast to the aldosterone-induced MR cistrome in a human renal cell line, where the majority of binding sites lack a GRE (26). The MR-exclusive sites had a more degenerate GRE (lower probability of bases) than the GR-exclusive sites. All subsets also contained a motif that matched the ZNF263 binding site, which was present in 18-67% of the sequences. The MR-GR overlapping sites all contained a motif that resembles a GRE half site, suggestive of concomitant dimeric and monomeric (or multimeric) binding of the receptors.

Interestingly, we found a distinct motif near the MR-exclusive sites, that was not enriched near the GR-exclusive or overlapping sites. This additional motif was present in 100% of the MR sites and matched to the Atoh1 binding sequence in the motif database. In a directed search, the Atoh1 motif was also enriched in MR over GR binding (AME, $p = 1.11 \times 10^{-24}$), although in individual cases we observed this site near GR-bound GREs (MAST, 1% of the GR-exclusive sites). The distance between the GRE and Atoh motif was normally distributed (**Figure 1C**) and independent of their respective orientation/strand (in or out of phase) or the binding site relative to genes (intergenic versus intragenic) (**Supplemental Figure 1C**). We supposed that another protein binding to this Atoh site can drive MR-specific binding.

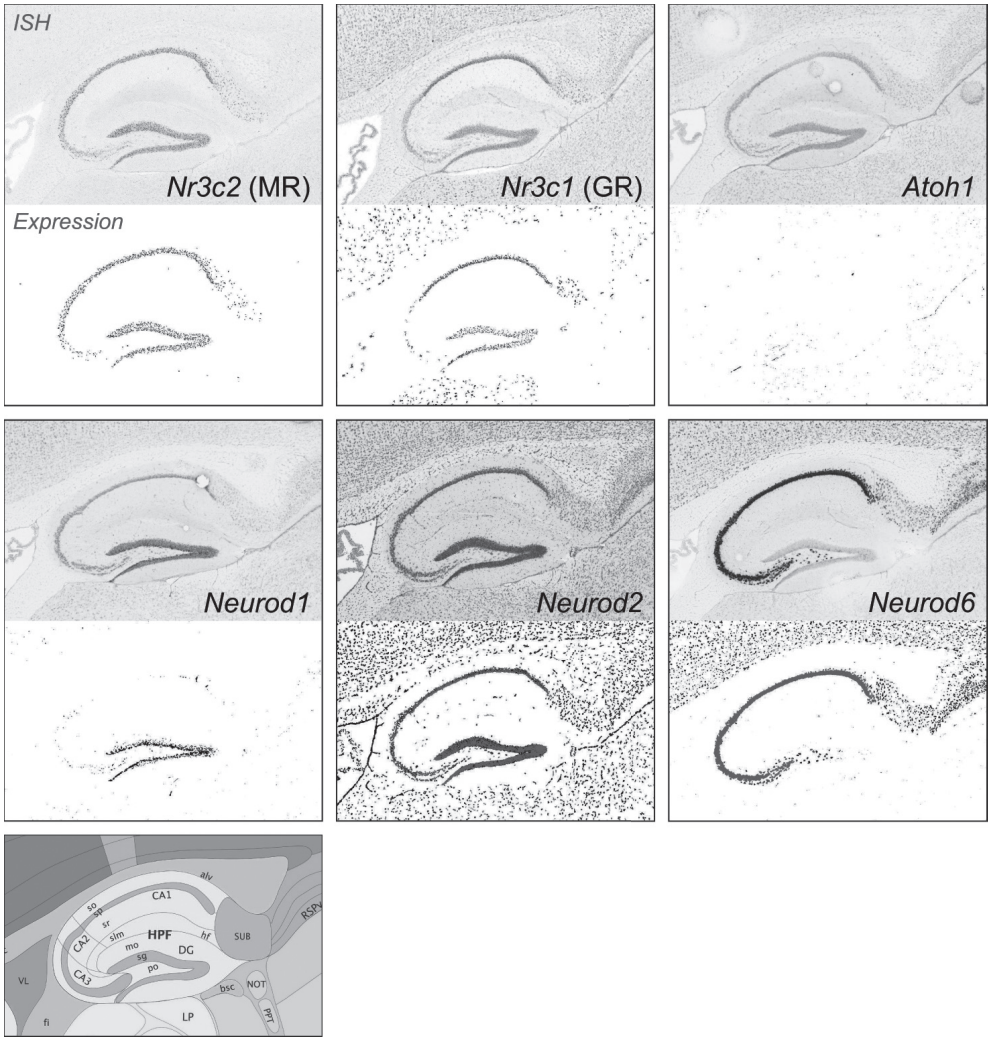


**Figure 3.** Expression of MR, GR, Atoh1 and NeuroD family members in the adult mouse hippocampus, with the corresponding reference atlas. Visualizations of the sagittal *in situ* hybridization (ISH) experiments and corresponding background subtracted signals (Expression) from the Allen Brain Atlas (24). Experiment_position numbers of depicted images are listed in the Supplemental Methods.

## NeuroD family members as candidate binders

According to the Allen Brain Atlas (24), *Atoh1* is not expressed in the mouse hippocampus (**Figure 3** and **Table 1**) and is therefore not considered a candidate to bind the MR-specific motif found in the hippocampal ChIP-seq dataset. Atoh1 belongs to the basic helix-loop-

helix (bHLH) family of transcription factors (27). Brain-specific family members *Neurod1*, *Neurod2* and *Neurod6* do show evident hippocampal expression (**Figure 3**) and have been shown to bind the identified CAGATGG motif (28-30). We validated the very low expression levels (or absence) of *Atoh1* and expression of the three NeuroD genes in the rat hippocampus by RT-qPCR (**Table 1**) and hypothesized (one of) these corresponding proteins could be responsible for the binding site selectivity for MR.

**Table 1**. Overview of Atoh1 and NeuroD family members and validation of mRNA expression levels in rat hippocampus.

| Protein | Synonyms | Expression peak | Adult hippocampal expression | | |
|---|---|---|---|---|---|
| | | | Subregion | ABA | Ct |
| **Atoh1** | Hath1, Math1, bHLHa14 | Early embryonic | - | 0.24 | >33.0 |
| **Neurod1** | BETA2, BHF-1, Neurod, bHLHa3 | E16-P0 * | Both CA & DG (higher in DG) | 1.41 | 23.2 |
| **Neurod2** | Ndrf, bHLHa1 | Stable throughout development * | Both CA & DG | 10.41 | 22.0 |
| **Neurod3** | Neurog1, AKA, Math4C, bHLHa6, Ngn1 | Early embryonic | - | 0.29 | - |
| **Neurod4** | AI846749, ATH-3, Atoh3, Math3, bHLHa4 | Early embryonic | - | 0.12 | - |
| **Neurod5** | Atoh6 | - | - | - | - |
| **Neurod6** | Atoh2, Math2, Nex, Nex1m, bHLHa2 | P5 * | CA1-CA3 | 11.73 | 21.0 |

The effect of Neurod1, Neurod2 and Neurod6 (grey rows) on glucocorticoid signaling was studied *in vitro*. ABA = Allen Brain Atlas, raw expression value in adult mouse hippocampal formation, β-actin = 21.17; as a reference MR = 0.68, GR = 2.18. The threshold cycle (Ct) values represent RT-qPCR measurements on 5 ng/μL cDNA, Sprague Dawley rat whole hippocampus, β-actin = 17.8. *(50)

By ChIP-qPCR we demonstrated Neurod2 binding at the same sites at which we validated MR binding (**Figure 2B**). It was however absent from GR-exclusive loci. This gives a proof of concept that Neurod2 might be binding to the Atoh site *in vivo*. While Neurod2 was selected based on the availability of ChIP-grade antibodies, this result does not exclude involvement of Neurod1 or Neurod6 in MR-selective signaling.

## In vivo co-expression of NeuroD factors with putative MR/GR target genes

To get an indication if the other two NeuroD factors could be (co-)responsible for the MR-selective binding *in vivo*, we examined to what extent they are co-expressed with putative MR/GR target genes (as defined by intragenic or up to -5kb binding of MR or GR). We assessed the spatial co-expression of the MR, overlapping and GR target gene lists with each of the NeuroD family members based on their expression patterns across the brain using data from the Allen Brain Atlas (24). The MR targets had a stronger co-expression with *Neurod6* than the overlapping or GR targets, while for *Neurod2* there was no difference between the three lists and the *Neurod1* spatial correlation was highest for the GR targets (**Supplemental Figure 3**). This could argue for Neurod6 as an *in vivo* determinant of MR-selective signaling. Nevertheless, all three NeuroD factors correlated strongly with the expression of MR-exclusive targets and were subsequently studied *in vitro*.

## NeuroD family members potentiate MR/GR transactivation

The putative role of Neurod1, Neurod2 and Neurod6 in MR-specific signaling was further studied in reporter assays in HEK293 cells. All three proteins potentiated MR, but unexpectedly also GR transactivation upon corticosterone treatment on a luciferase construct containing a GRE plus the additional Atoh motif in its promoter (GRE-At), by approximately 4-fold and 7- to 9-fold, respectively (**Figure 4**). This effect was not observed at a control construct lacking the Atoh binding site (GRE-MutAt), and the NeuroDs could not enhance reporter expression without hormone stimulation. The NeuroD factors thus acted as MR/GR transcriptional coactivators via the identified Atoh motif. For Neurod6, a clear dose-response curve was observed for transfection with increasing doses of expression vector (**Supplemental Figure 4A**). We further tested a reporter driven by a more degenerate GRE, as found for the MR-exclusive sites (**Figure 1B**), combined with the additional Atoh site (MRE-At). The receptors were less efficient in stimulating this luciferase promoter and the NeuroD effect also did not differ for MR and GR on this reporter (**Supplemental Figure 4B**).

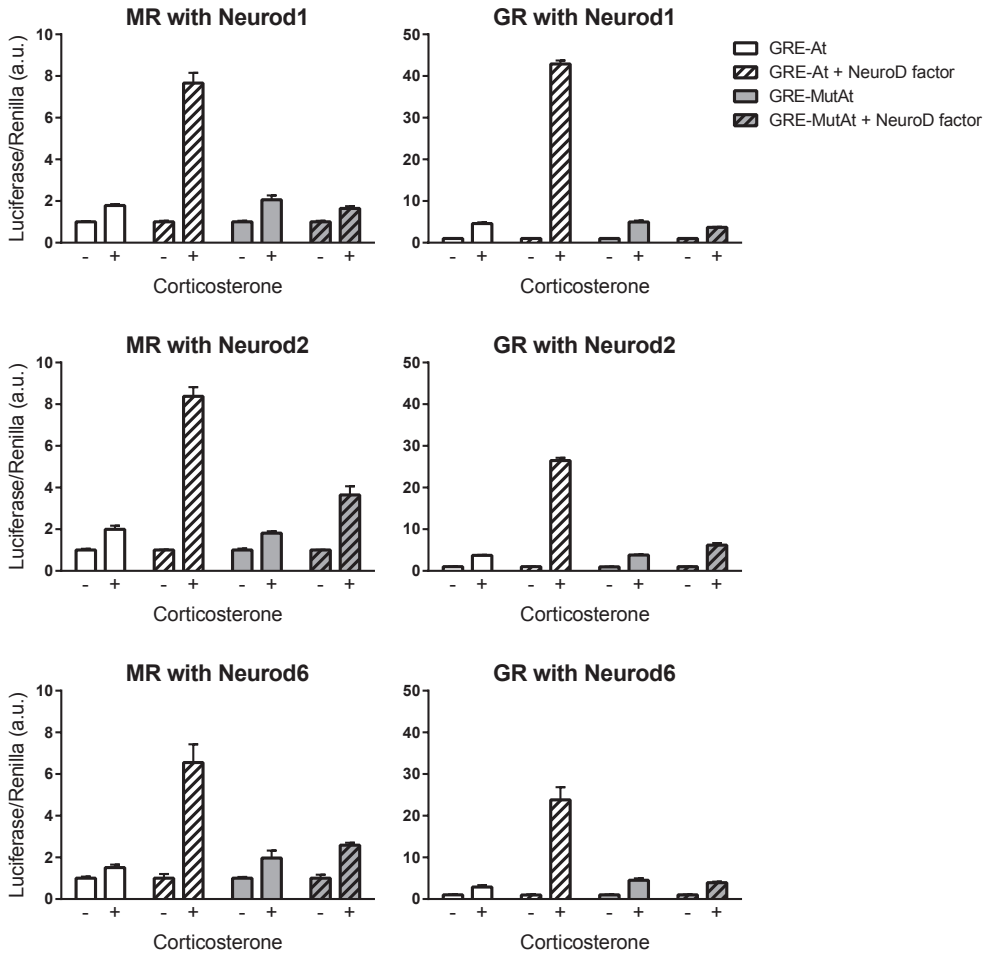


**Figure 4**. Potentiation of MR and GR transactivation by NeuroD family members on a luciferase construct containing a perfect GRE plus the additional MR-exclusive motif. HEK293 cells were transfected with MR or GR; the GRE-At or GRE-MutAt luciferase constructs; Neurod1, Neurod2 or Neurod6 (10 ng/well) and stimulated with corticosterone ($10^{-7}$ M). Non-stimulated cells were normalized to 1. a.u. = arbitrary unit

## NeuroD family members increase mainly the maximum transcriptional effect

As the mechanism of action of a receptor modulator can be deduced from both the change in maximum effect, as well as the ligand concentration needed for 50% of this effect (EC50) (31), we generated corticosterone dose-response curves with and without co-transfecting

Neurod6. The maximum MR/GR effect was increased by Neurod6 presence over the whole concentration range that activates the receptor (data not shown), as was seen before by increased luciferase expression at saturating corticosterone concentrations of $10^{-7}$ M (**Figure 4**). Besides, the EC50 was not changed for MR ($2.24\pm0.06 \times 10^{-10}$ M versus $1.89\pm0.05 \times 10^{-10}$ M), while the GR showed a slightly decreased EC50 upon Neurod6 addition ($1.03\pm0.05 \times 10^{-8}$ M versus $5.29\pm0.02 \times 10^{-9}$ M) (**Figure 5A**).

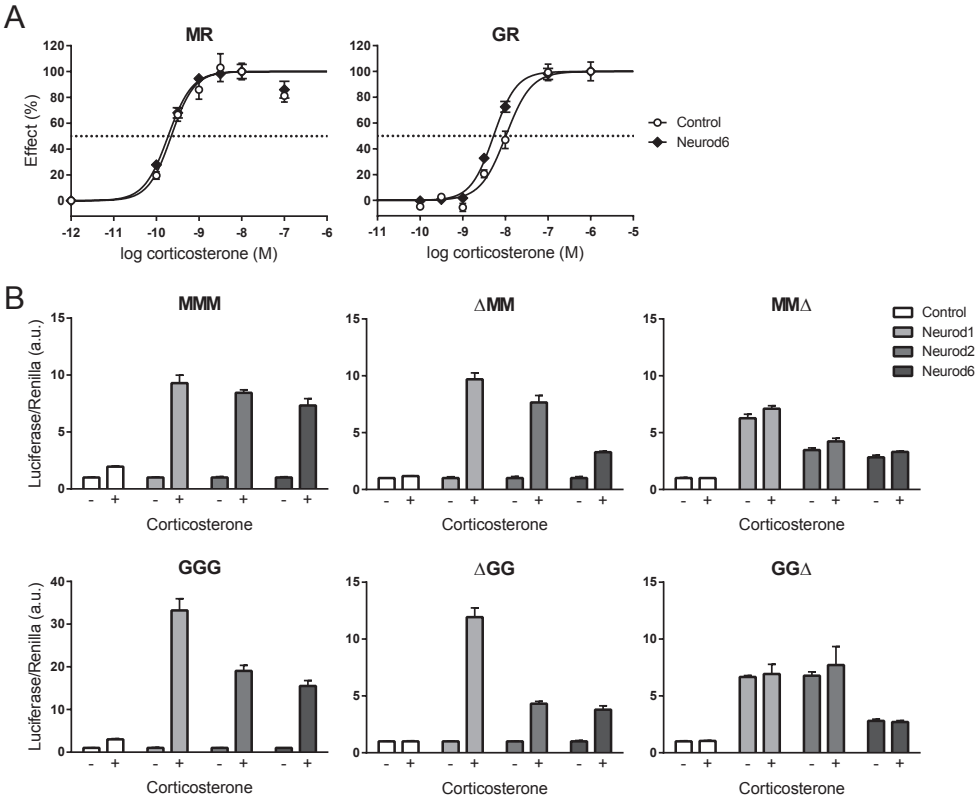


**Figure 5**. NeuroD increases the maximum MR/GR effect via an indirect mechanism of action. **A)** Dose-response curves for corticosterone stimulation of MR and GR in absence and presence of Neurod6, to determine the effect on EC50. The luciferase activity is presented as percentage of the maximum effect. Sigmoidal curves were fit by non-linear regression using a variable slope model. **B)** Effect of NeuroD factors on truncated receptors. HEK293 cells were transfected with full MR or GR (MMM, GGG) or variants lacking the N-terminus (ΔMM, ΔGG) or C-terminus (MMΔ, GGΔ); the GRE-At construct; Neurod1, Neurod2 or Neurod6 (10 ng/well) and stimulated with corticosterone ($10^{-7}$ M). All non-stimulated cells were normalized to 1; for the constitutively active MMΔ and GGΔ luciferase levels were normalized to non-stimulated control cells. a.u. = arbitrary unit

### NeuroD family members interact with both N-terminal and C-terminal domain lacking receptors

To further investigate the mechanism of interaction between the MR/GR and NeuroD factors, reporter assays were performed using truncated receptors (**Figure 5B**). The transactivation by receptors lacking the LBD (MM∆ and GG∆) could be potentiated by the different NeuroDs, although to a lesser extent than for the full-length receptors (MMM and GGG). The potentiation by NeuroDs was also seen without hormone treatment for these constitutively active receptors lacking the LBD. Besides, the NeuroDs could also increase transcriptional activity of the receptors that did not have an N-terminal domain (∆MM and ∆GG). For MR the NeuroD potentiation of the truncate was comparable to that for the full length receptor, but for GR the enhancement relative to non-stimulated cells was less than half that of the full length receptor. Unexpectedly, the ∆MM and ∆GG were unresponsive to corticosterone treatment at this reporter, but we did confirm proper transactivation at TAT1-Luc and TAT3-Luc reporters (data not shown). This potentiation of both N- and C-terminal receptor truncations suggests that NeuroD factors have an indirect interaction with MR/GR.



## Discussion

This study examined the overlap and specificity of MR versus GR regarding whole genome hippocampal binding sites. We found both MR-specific, GR-specific and joint sites, that all contained a GRE. Virtually all MR-specific sites had an Atoh consensus sequence within 400 bp of the GRE, whereas *de novo* motif analysis did not find this sequence near sites that showed GR occupancy (including overlapping sites). Neurod1, Neurod2 and Neurod6 are co-expressed with MR and/or GR in the principal hippocampal cell layers, and all could act as coactivators of both MR and GR in reporter assays.

The limited overlap found in MR and GR binding sites is in accordance with the distinct roles of the two receptors in the hippocampus (6, 10, 32). It should be noted however that the lower sequencing depth of our analysis might have precluded the detection of weaker binding sites. In addition, as we performed ChIP-seq on whole hippocampi, the small proportion of shared targets could also be a result of cell type specific MR/GR loci as a consequence of the differential MR and GR expression patterns throughout the hippocampal area. Co-expression of MR and GR is observed in the majority of CA pyramidal and dentate gyrus granular neurons, with the exception of CA3 pyramidal cells that have high MR but low GR levels (33). Besides GR is also expressed in glial cells (34, 35).

Limited overlap in the MR binding sites for the two different corticosterone doses (MR300 versus MR3000) could be explained partly by an insufficient depth of sequencing (limit of detection). In addition it might reflect different concentrations of activated MR in the nucleus, in combination with differential affinity of binding sequences for the receptor – even if the majority of MR likely was occupied by the lower dose. A recent study suggests that high receptor occupancy does not necessarily translate into high DNA binding, and MR can show circadian variation in target site occupancy (36). Differences in sensitivity between MR-expressing cell types might also be of relevance. A last possibility may be opening up of chromatin domains via GR, making GREs available for MR binding. In the same line, heterodimerization of MR and GR could play a role (36).

The additional, MR-selective motif could be bound by Neurod1, Neurod2 and Neurod6, as evidenced by response-element dependent transcriptional modulation. NeuroD proteins are members of the bHLH protein family and are known for their function in neuronal differentiation (28, 37). *Neurod1* knockout mice lack a dentate granule cell layer (38), and heterozygous *Neurod2* deficient mice show impaired contextual and cued freezing in a fear-conditioning task (29). Our binding sites were detected in adult rat hippocampal tissue, suggesting that the NeuroD factors not only regulate neuronal differentiation during development, but also can be crucial in later processes such as cell survival or retaining differentiation status. As the hippocampal dentate gyrus is the main site of adult neurogenesis (39), this might also provide a role for NeuroD factors in adulthood, although their expression is much wider than neurogenic zones. Furthermore, overexpression of Neurod2 in the ventral hippocampus has recently been shown to increase stress susceptibility in a chronic social defeat paradigm (40), posing a role for Neurod2 in depression.

Based on mouse brain expression data from the Allen Brain Atlas, we observed that *Neurod6* expression is restricted to the CA subregions of the hippocampus, while the lower *Neurod1* signal seems to be more pronounced in the DG (**Figure 3**). Furthermore, *Neurod2* expression is observed throughout the whole hippocampus and seems to be at levels similar to *Neurod6*, as we validated by RT-qPCR on rat hippocampal tissue. The three NeuroD proteins have a highly similar bHLH region (37), which makes it not surprising that all members can bind the additional Atoh motif derived from our ChIP-seq analysis and potentiate MR/GR transactivation in reporter assays. Based on our data we cannot pinpoint which of the family members is/are responsible for the MR specific binding, although Neurod2 was detected at rat hippocampal MR-exclusive sites (**Figure 2B**) and target gene correlations suggest that Neurod6 is also a likely candidate (**Supplemental**

**Figure 3**). We cannot exclude the possibility that another bHLH containing protein binds to the Atoh motif and drives the exclusive MR action. *Neurod1* or *Neurod2* deficient mice that also lack *Neurod6* have more severe brain abnormalities than the single mutants, indicating cooperation and/or partial redundancy (41, 42). A model in which Neurod1, Neurod2 and Neurod6 are each involved in MR-specific signaling within a certain subregion of the hippocampus might be considered.

The *in vivo* found MR-exclusive motif does not discriminate *in vitro* in reporter assays. This discrepancy could be explained by the possibility that in the luciferase assay the receptors use different intermediate transcriptional proteins than in the hippocampus. The observed coactivation of both N- and C-terminally truncated receptors implies that NeuroD family members interact via the transcriptional complex of MR/GR rather than directly with the receptors. A side note is that we cannot rule out interactions via the DBD or hinge region of the receptors. Nevertheless, the suggested indirect interaction is also supported by the fact that the Atoh motif was found at a variable distance up to 400 bp from the GRE. It is likely that the HEK293 cells lack or do contain other variants of the proteins that are crucial to mediate the NeuroD effect on selective MR transcriptional activity. For example, the pool of coregulators present in a cell is highly tissue-specific and can result in opposite effects on gene transcription (43). Also, bHLH protein heterodimerization partners might be responsible for an MR specific effect (27). Besides, as the chromatin landscape is a crucial determinant of a transcription factor cistrome (44), the lack of chromatin context in the luciferase assay might make it difficult to mimic the exact conditions of *in vivo* binding and transcription. Interestingly, Neurod1 itself can also induce chromatin remodeling and increase neuronal gene accessibility (45).

In lung fibroblasts, the Atoh1 motif was detected, although non-significantly, near GR-bound sequences (46). Directed motif search by MAST showed the presence of a Neurod2 binding site in 1% of our GR-exclusive sites, but the Atoh motif was clearly enriched in MR- over GR-exclusive sites using AME. It might be that a NeuroD factor through binding to the Atoh motif only excludes GR binding and subsequent transactivation when MR is present, which can be another reason that we do not find a difference in MR/GR potentiation *in vitro* when studying the receptors in isolation. In co-transfections of MR and GR combined with selective pharmacological activation, also both receptors were potentiated by Neurod6 (data not shown). Furthermore, the highly dynamic DNA binding kinetics of nuclear receptors are not supportive of a competition based mechanism (47, 48). A recent study also found motifs that were associated with absence of GR binding,

and proteins recognizing these sequences could indeed decrease GR occupancy and transactivation (49).

In conclusion, we identified a motif that is associated with MR-selective signaling in the rat hippocampus. NeuroD factors could bind this motif and via indirect interactions were found to potentiate the MR/GR transcriptional activity in HEK293 cells. The data support a model in which NeuroD factors stabilize MR binding *in vivo* by interacting with cell specific components of the MR-associated transcriptional complex. Further elucidation of distinct MR/GR downstream pathways will enable us to more specifically target aspects of glucocorticoid signaling for treatment of stress-related disorders.

## Acknowledgements

We thank Robin Schoonderwoerd for technical assistance. We gratefully acknowledge Dr. Mitsuhiko Yamada and Dr. David Pearce for providing plasmids. This research was supported by NWO ALW grant 823.02.002 and COST Action ADMIRE BM1301.

# References


1. de Kloet ER, Joels M, Holsboer F. Stress and the brain: from adaptation to disease. Nature reviews Neuroscience. 2005;6(6):463-75.
2. Reul JM, de Kloet ER. Two receptor systems for corticosterone in rat brain: microdistribution and differential occupation. Endocrinology. 1985;117(6):2505-11.
3. de Kloet ER, Otte C, Kumsta R, Kok L, Hillegers MH, Hasselmann H, et al. Stress and Depression: a Crucial Role of the Mineralocorticoid Receptor. Journal of neuroendocrinology. 2016;28(8).
4. Joels M, Karst H, DeRijk R, de Kloet ER. The coming out of the brain mineralocorticoid receptor. Trends in neurosciences. 2008;31(1):1-7.
5. Vogel S, Fernandez G, Joels M, Schwabe L. Cognitive Adaptation under Stress: A Case for the Mineralocorticoid Receptor. Trends in cognitive sciences. 2016;20(3):192-203.
6. Oitzl MS, de Kloet ER. Selective corticosteroid antagonists modulate specific aspects of spatial orientation learning. Behavioral neuroscience. 1992;106(1):62-71.
7. Roozendaal B. Stress and memory: opposing effects of glucocorticoids on memory consolidation and memory retrieval. Neurobiology of learning and memory. 2002;78(3):578-95.
8. Sapolsky RM, Romero LM, Munck AU. How do glucocorticoids influence stress responses? Integrating permissive, suppressive, stimulatory, and preparative actions. Endocrine reviews. 2000;21(1):55-89.
9. Joels M, Sarabdjitsingh RA, Karst H. Unraveling the time domains of corticosteroid hormone influences on brain activity: rapid, slow, and chronic modes. Pharmacological reviews. 2012;64(4):901-38.
10. Joels M, de Kloet ER. Mineralocorticoid receptor-mediated changes in membrane properties of rat CA1 pyramidal neurons in vitro. Proceedings of the National Academy of Sciences of the United States of America. 1990;87(12):4495-8.
11. De Bosscher K, Vanden Berghe W, Haegeman G. The interplay between the glucocorticoid receptor and nuclear factor-kappaB or activator protein-1: molecular mechanisms for gene repression. Endocrine reviews. 2003;24(4):488-522.
12. Polman JA, de Kloet ER, Datson NA. Two populations of glucocorticoid receptor-binding sites in the male rat hippocampal genome. Endocrinology. 2013;154(5):1832-44.
13. Liu W, Wang J, Sauter NK, Pearce D. Steroid receptor heterodimerization demonstrated in vitro and in vivo. Proceedings of the National Academy of Sciences of the United States of America. 1995;92(26):12480-4.
14. Trapp T, Holsboer F. Heterodimerization between mineralocorticoid and glucocorticoid receptors increases the functional diversity of corticosteroid action. Trends in pharmacological sciences. 1996;17(4):145-9.
15. Zalachoras I, Houtman R, Meijer OC. Understanding stress-effects in the brain via transcriptional signal transduction pathways. Neuroscience. 2013;242:97-109.
16. Arriza JL, Weinberger C, Cerelli G, Glaser TM, Handelin BL, Housman DE, et al. Cloning of human mineralocorticoid receptor complementary DNA: structural and functional kinship with the glucocorticoid receptor. Science. 1987;237(4812):268-75.
17. Zhang Y, Liu T, Meyer CA, Eeckhoute J, Johnson DS, Bernstein BE, et al. Model-based analysis of ChIP-Seq (MACS). Genome biology. 2008;9(9):R137.

18. Robinson JT, Thorvaldsdottir H, Winckler W, Guttman M, Lander ES, Getz G, et al. Integrative genomics viewer. Nature biotechnology. 2011;29(1):24-6.
19. Heinz S, Benner C, Spann N, Bertolino E, Lin YC, Laslo P, et al. Simple combinations of lineage-determining transcription factors prime cis-regulatory elements required for macrophage and B cell identities. Molecular cell. 2010;38(4):576-89.
20. Huang da W, Sherman BT, Lempicki RA. Systematic and integrative analysis of large gene lists using DAVID bioinformatics resources. Nature protocols. 2009;4(1):44-57.
21. Bailey TL, Boden M, Buske FA, Frith M, Grant CE, Clementi L, et al. MEME SUITE: tools for motif discovery and searching. Nucleic acids research. 2009;37(Web Server issue):W202-8.
22. Yamada M, Shida Y, Takahashi K, Tanioka T, Nakano Y, Tobe T, et al. Prg1 is regulated by the basic helix-loop-helix transcription factor Math2. Journal of neurochemistry. 2008;106(6):2375-84.
23. Pearce D, Yamamoto KR. Mineralocorticoid and glucocorticoid receptor activities distinguished by nonreceptor factors at a composite response element. Science. 1993;259(5098):1161-5.
24. Lein ES, Hawrylycz MJ, Ao N, Ayres M, Bensinger A, Bernard A, et al. Genome-wide atlas of gene expression in the adult mouse brain. Nature. 2007;445(7124):168-76.
25. Mahfouz A, Lelieveldt BP, Grefhorst A, van Weert LT, Mol IM, Sips HC, et al. Genome-wide coexpression of steroid receptors in the mouse brain: Identifying signaling pathways and functionally coordinated regions. Proceedings of the National Academy of Sciences of the United States of America. 2016;113(10):2738-43.
26. Le Billan F, Khan JA, Lamribet K, Viengchareun S, Bouligand J, Fagart J, et al. Cistrome of the aldosterone-activated mineralocorticoid receptor in human renal cells. FASEB journal : official publication of the Federation of American Societies for Experimental Biology. 2015;29(9):3977-89.
27. Massari ME, Murre C. Helix-loop-helix proteins: regulators of transcription in eucaryotic organisms. Molecular and cellular biology. 2000;20(2):429-40.
28. Fong AP, Yao Z, Zhong JW, Cao Y, Ruzzo WL, Gentleman RC, et al. Genetic and epigenetic determinants of neurogenesis and myogenesis. Developmental cell. 2012;22(4):721-35.
29. Lin CH, Hansen S, Wang Z, Storm DR, Tapscott SJ, Olson JM. The dosage of the neuroD2 transcription factor regulates amygdala development and emotional learning. Proceedings of the National Academy of Sciences of the United States of America. 2005;102(41):14877-82.
30. Poulin G, Turgeon B, Drouin J. NeuroD1/beta2 contributes to cell-specific transcription of the proopiomelanocortin gene. Molecular and cellular biology. 1997;17(11):6673-82.
31. Simons SS, Jr., Chow CC. The road less traveled: new views of steroid receptor action from the path of dose-response curves. Molecular and cellular endocrinology. 2012;348(2):373-82.
32. Joels M, de Kloet ER. Coordinative mineralocorticoid and glucocorticoid receptor-mediated control of responses to serotonin in rat hippocampus. Neuroendocrinology. 1992;55(3):344-50.
33. Van Eekelen JA, de Kloet ER. Co-localization of brain corticosteroid receptors in the rat hippocampus. Progress in histochemistry and cytochemistry. 1992;26(1-4):250-8.
34. Nichols NR, Osterburg HH, Masters JN, Millar SL, Finch CE. Messenger RNA for glial fibrillary acidic protein is decreased in rat brain following acute and chronic corticosterone treatment. Brain research Molecular brain research. 1990;7(1):1-7.
35. Vielkind U, Walencewicz A, Levine JM, Bohn MC. Type II glucocorticoid receptors are expressed in oligodendrocytes and astrocytes. Journal of neuroscience research. 1990;27(3):360-73.
36. Mifsud KR, Reul JM. Acute stress enhances heterodimerization and binding of corticosteroid receptors at glucocorticoid target genes in the hippocampus. Proceedings of the National Academy of Sciences of the United States of America. 2016;113(40):11336-41.

37. Hassan BA, Bellen HJ. Doing the MATH: is the mouse a good model for fly development? Genes & development. 2000;14(15):1852-65.

38. Liu M, Pleasure SJ, Collins AE, Noebels JL, Naya FJ, Tsai MJ, et al. Loss of BETA2/NeuroD leads to malformation of the dentate gyrus and epilepsy. Proceedings of the National Academy of Sciences of the United States of America. 2000;97(2):865-70.

39. Fitzsimons CP, van Hooijdonk LW, Schouten M, Zalachoras I, Brinks V, Zheng T, et al. Knockdown of the glucocorticoid receptor alters functional integration of newborn neurons in the adult hippocampus and impairs fear-motivated behavior. Molecular psychiatry. 2013;18(9):993-1005.

40. Bagot RC, Cates HM, Purushothaman I, Lorsch ZS, Walker DM, Wang J, et al. Circuit-wide Transcriptional Profiling Reveals Brain Region-Specific Gene Networks Regulating Depression Susceptibility. Neuron. 2016;90(5):969-83.

41. Bormuth I, Yan K, Yonemasu T, Gummert M, Zhang M, Wichert S, et al. Neuronal basic helix-loop-helix proteins Neurod2/6 regulate cortical commissure formation before midline interactions. The Journal of neuroscience : the official journal of the Society for Neuroscience. 2013;33(2):641-51.

42. Schwab MH, Bartholomae A, Heimrich B, Feldmeyer D, Druffel-Augustin S, Goebbels S, et al. Neuronal basic helix-loop-helix proteins (NEX and BETA2/Neuro D) regulate terminal granule cell differentiation in the hippocampus. The Journal of neuroscience : the official journal of the Society for Neuroscience. 2000;20(10):3714-24.

43. Lachize S, Apostolakis EM, van der Laan S, Tijssen AM, Xu J, de Kloet ER, et al. Steroid receptor coactivator-1 is necessary for regulation of corticotropin-releasing hormone by chronic stress and glucocorticoids. Proceedings of the National Academy of Sciences of the United States of America. 2009;106(19):8038-42.

44. John S, Sabo PJ, Thurman RE, Sung MH, Biddie SC, Johnson TA, et al. Chromatin accessibility pre-determines glucocorticoid receptor binding patterns. Nature genetics. 2011;43(3):264-8.

45. Pataskar A, Jung J, Smialowski P, Noack F, Calegari F, Straub T, et al. NeuroD1 reprograms chromatin and transcription factor landscapes to induce the neuronal program. The EMBO journal. 2016;35(1):24-45.

46. Starick SR, Ibn-Salem J, Jurk M, Hernandez C, Love MI, Chung HR, et al. ChIP-exo signal associated with DNA-binding motifs provides insight into the genomic binding of the glucocorticoid receptor and cooperating transcription factors. Genome research. 2015;25(6):825-35.

47. Groeneweg FL, van Royen ME, Fenz S, Keizer VI, Geverts B, Prins J, et al. Quantitation of glucocorticoid receptor DNA-binding dynamics by single-molecule microscopy and FRAP. PloS one. 2014;9(3):e90532.

48. Voss TC, Schiltz RL, Sung MH, Yen PM, Stamatoyannopoulos JA, Biddie SC, et al. Dynamic exchange at regulatory elements during chromatin remodeling underlies assisted loading mechanism. Cell. 2011;146(4):544-54.

49. Telorac J, Prykhozhij SV, Schone S, Meierhofer D, Sauer S, Thomas-Chollier M, et al. Identification and characterization of DNA sequences that prevent glucocorticoid receptor binding to nearby response elements. Nucleic acids research. 2016.

50. Schwab MH, Druffel-Augustin S, Gass P, Jung M, Klugmann M, Bartholomae A, et al. Neuronal basic helix-loop-helix proteins (NEX, neuroD, NDRF): spatiotemporal expression and targeted disruption of the NEX gene in transgenic mice. The Journal of neuroscience : the official journal of the Society for Neuroscience. 1998;18(4):1408-18.

# Supplemental data

### Supplemental Methods

ChIP washing buffers

Low salt wash buffer (1x)
150 mM NaCl, 20 mM Tris-HCl pH 8.1, 2 mM EDTA, 0.1% SDS, 1% Triton X-100
High salt wash buffer (1x)
500 mM NaCl, 20 mM Tris-HCl pH 8.1, 2 mM EDTA, 0.1% SDS, 1% Triton X-100
LiCl wash buffer (1x)
10 mM Tris-HCl pH 8.1, 1 mM EDTA, 0.25 M LiCl, 1% NP-40, 1% deoxycholate
TE wash buffer (2x)
M Tris-HCl pH 8.0, 1 mM EDTA

Allen Brain Atlas experiment_position numbers used for Figure 2

*Nr3c2* (MR): 731_91
*Nr3c1* (GR): 728_102
*Atoh1*: 75826683_96
*Neurod1*: 79632311_96
*Neurod2*: 70437810_98
*Neurod6*: 79544834_101

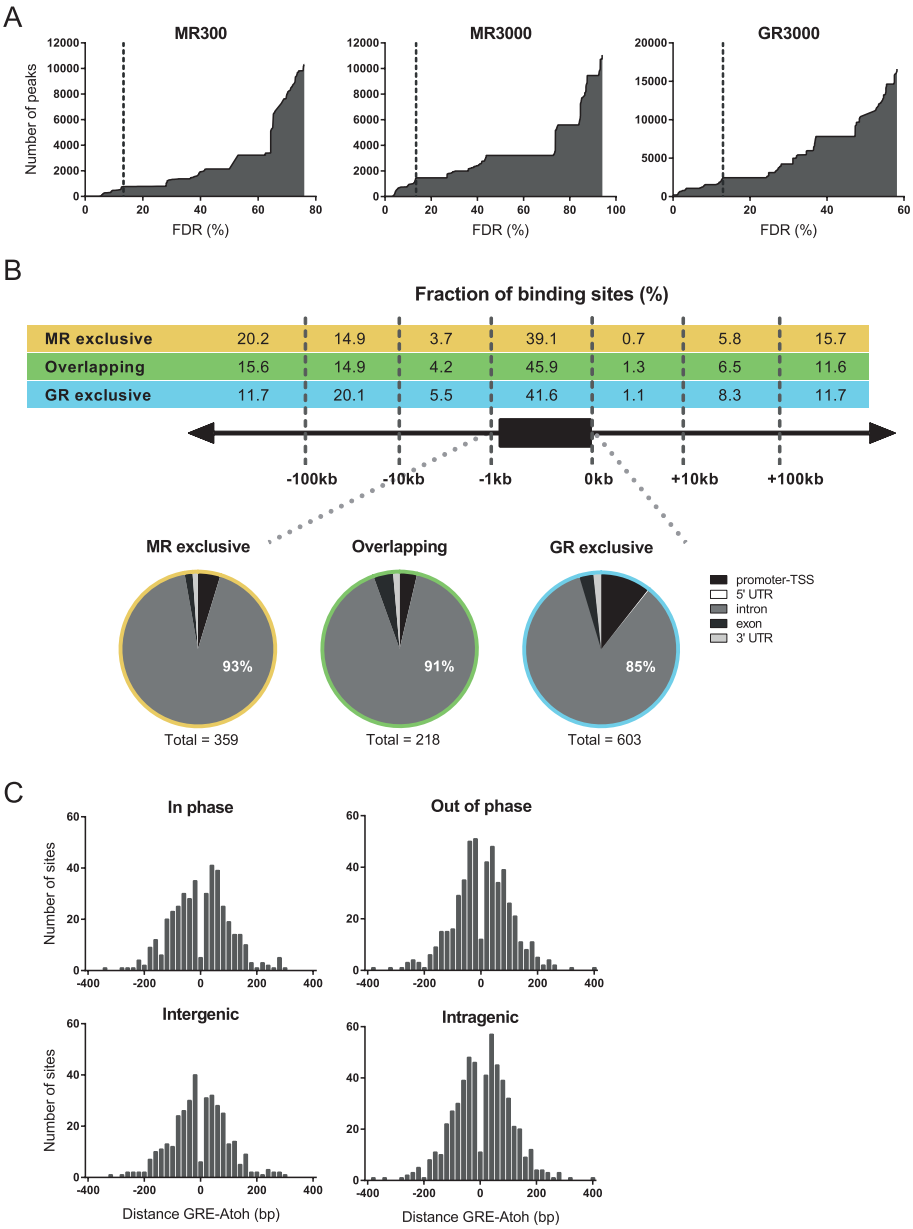


**Supplemental Figure 1**. ChIP-seq binding site analysis. **A)** FDR distribution across called peaks, with evident gaps from 13.33-28.12% for MR300, 13.49-26.88% for MR3000 and 12.98-24.08% for GR3000 datasets. Based on this 13.5% was set as FDR cutoff. **B)** Genomic distribution of MR, overlapping or GR binding sites relative to the nearest gene. Insets show detailed locations of intragenic (promoter-TSS, intron, exon, UTR) binding sites. Promoter-TSS is defined as -1kb to +100bp. **C)** Effect of relative motif orientation and location relative to genes on distribution of distance between GRE and Atoh motifs. Motifs were found both on the same strand (in phase) or on the opposite strands (out of phase). TSS = transcription start site, UTR = untranslated region

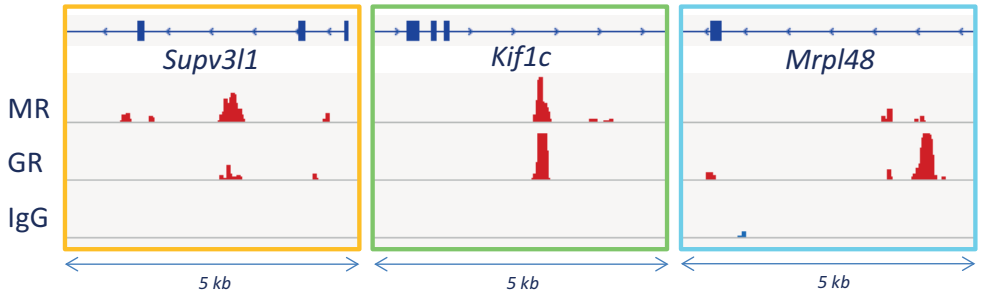


**Supplemental Figure 2**. IGV browser screenshots showing examples of an intragenic MR-exclusive (*Supv3l1*), overlapping (*Kif1c*) and GR-exclusive (*Mrpl48*) binding site.

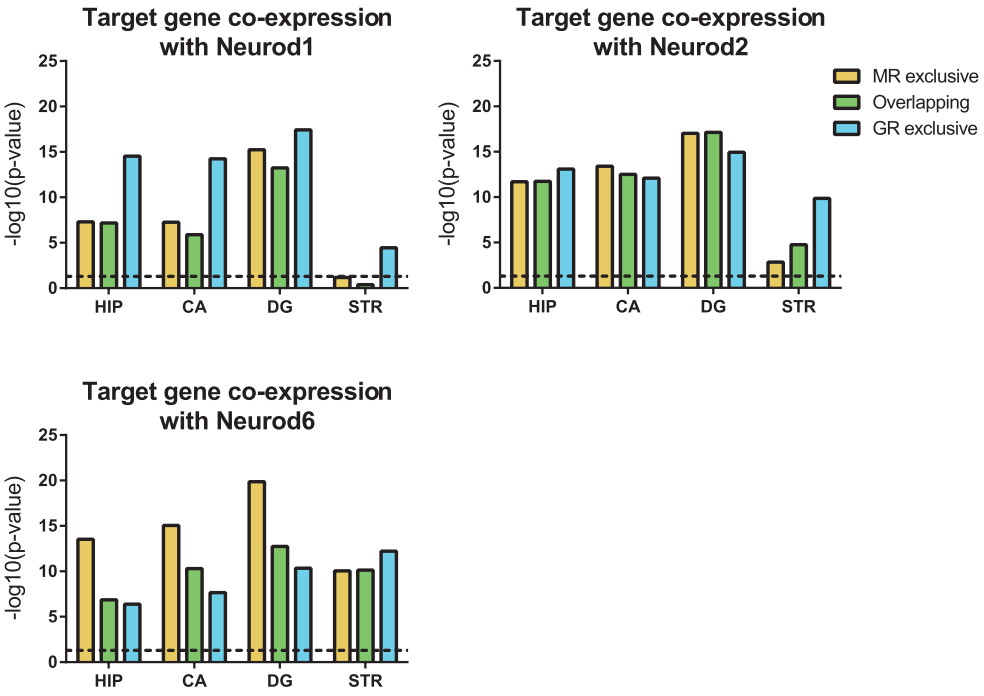


**Supplemental Figure 3**. Target gene list co-expression. Correlation of target genes with NeuroD family member expression for the whole hippocampus (HIP), CA and DG subregions and striatum (STR) as control region. Logarithm of the Wilcoxon rank-sum test p-value. Dashed lines represent the significance level.

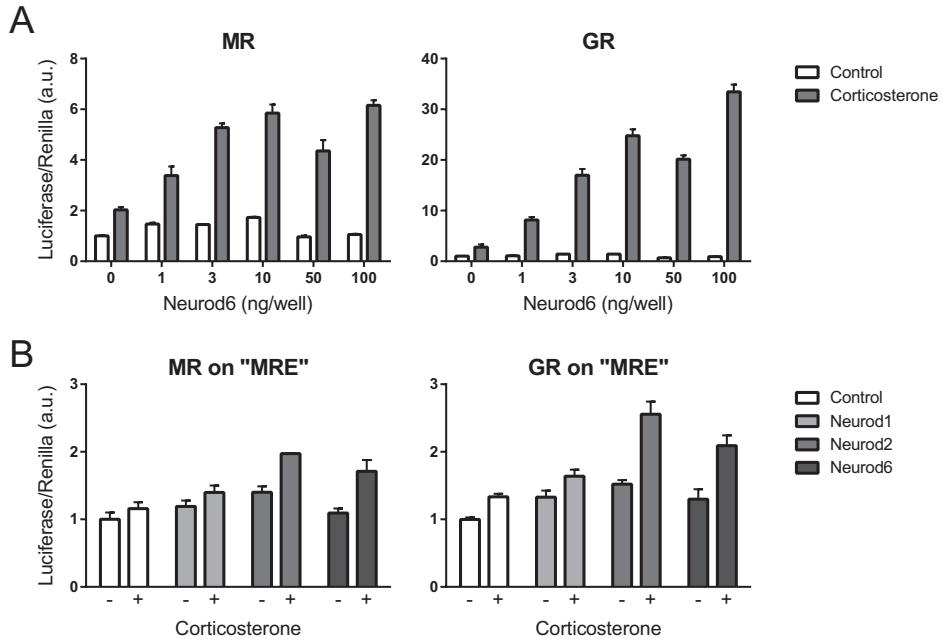


**Supplemental Figure 4**. **A)** Dose-response curve of Neurod6 transfection on GRE-At construct. **B)** Effect of NeuroD on a luciferase construct containing a more degenerate GRE plus the additional MR-exclusive motif. HEK293 cells were transfected with MR or GR; the MRE-At luciferase construct; Neurod1, Neurod2 or Neurod6 (10 ng/well) and stimulated with corticosterone ($10^{-7}$ M). Luciferase levels were normalized to non-stimulated control cells.

**Supplemental Table 1**. Antibodies used for ChIP.

| Target | Antigen sequence | Name | Manufacturer, catalog number | Species raised in, clonality | RRID |
|---|---|---|---|---|---|
| MR | Amino acids 1-300 of human MR | MR antibody (H-300) X | Santa Cruz Biotechnology, sc-11412X | Rabbit polyclonal IgG | AB_2155949 |
| GR | Amino acids 121-420 of human GR | GR antibody (H-300) X | Santa Cruz Biotechnology, sc-8992X | Rabbit polyclonal IgG | AB_2155784 |
| Neurod2 | Synthetic peptide of human NeuroD2 residues | NeuroD2 antibody [EPR5135] | Abcam, ab109406 | Rabbit monoclonal IgG | AB_10866309 |
| IgG | No known specificity | Isotype control | Abcam, ab37415 | Rabbit polyclonal IgG | AB_2631996 |

All antibodies were used in a dilution of 6 µg/500 µL.

**Supplemental Table 2**. Primer sequences used for ChIP-qPCR validation (upper list) and RT-qPCR on rat hippocampal cDNA (lower list). Mouse intestinal cDNA was used as a positive control to test the efficiency of Atoh1 primers.

| Binding site | Nearest gene | Forward & reverse (5'>3') | Product length (bp) |
|---|---|---|---|
| **MR300_116** | *Kcns1* | GGCCTTAGTGAAGGAACCAGG<br>ACTCACCATCTGCTCCTTGG | 153 |
| **MR300_196** | *Nos1ap* | GGTGTCTTTTTCTCTTCCCACAC<br>AAAGATAAGCAGACCAACCCA | 183 |
| **MR300_503** | *Rilpl1* | CAGGCAGATGCCAGGCT<br>CCCATGCCTGTTCCTCTAGT | 106 |
| **MR3000_359** | *Supv3l1* | TCTGTGTGTGACTGCCTGAC<br>CTCTCAGGGCTTCCCTGTTT | 111 |
| **GR3000_1726** | *Ascl6* | CCTGCCAGGAGAGCAGATG<br>TGTGCAGGAAGGCAAGTTCT | 178 |
| **GR3000_193** | *C4ST1* | ACCCTCTCTGAATGGACAGC<br>GTGGTTTGGCAGCCATCTTC | 179 |
| **GR3000_106** | *Mrpl48* | TGGACAGAGCTGTGCTTTGG<br>CACAGCAGCGCTGAGGTTTA | 151 |
| **Gene** | **Full name** | **Forward & reverse (5'>3')** | **Product length (bp)** |
| ***Actb*** | Beta-actin | TGAACCCTAAGGCCAACCGTG<br>ACACAGCCTGGATGGCTACG | 90 |
| ***Atoh1*** | Atonal bHLH transcription factor 1 | TCTGACGAGGCCAGTTAGGA<br>TCCGAAGTCACATCGTTGCT | 156 |
| ***Neurod1*** | Neuronal differentiation 1 | AGGTGGTACCCTGCTACTCT<br>GCTGGGACAAACCTTTGCAG | 159 |
| ***Neurod2*** | Neuronal differentiation 2 | TAAGGGGCTGCTGAGTTTCG<br>GGAGATTCGTGTTGGGGTGA | 160 |
| ***Neurod6*** | Neuronal differentiation 6 | AGAGGCTCCAGGAGACGATG<br>TGGGATTCGGGCATTACGAC | 155 |

**Supplemental Table 3**. Lists of MR, overlapping and GR binding sites. Available on https://doi.org/10.1210/en.2016-1422

**Supplemental Table 4**. Lists of MR, overlapping and GR target genes. In the MR-exclusive list, 35 of the MR300 binding sites have an overlapping MR3000 peak, which is listed under 'corresponding binding site'. Available on https://doi.org/10.1210/en.2016-1422

**Supplemental Table 5**. Gene ontology for MR, overlapping and GR target genes. The top 10 functional annotation clusters with an enrichment score (ES) above 1.3. The ES is the negative logarithm of the geometric mean of p-values from all terms within the cluster. BP = biological process, CC = cellular component, MF = molecular function

**MR-exclusive target genes**

| GO term(s) | Category | Enrichment score |
|---|---|---|
| **Nucleotide binding** | MF | 3.50 |
| **Ion transport, voltage-gated channel activity** | MF | 2.43 |
| **Sodium channel activity** | MF | 2.21 |
| **Ion homeostasis** | BP | 1.95 |
| **Immunoglobulin, cell adhesion** | BP | 1.78 |
| **Regulation of cell projection assembly** | BP | 1.72 |
| **Membrane/insoluble fraction** | CC | 1.69 |
| **Enzyme/kinase binding** | MF | 1.63 |
| **Endoplasmic reticulum** | CC | 1.53 |
| **Calcium ion transport/signaling** | BP | 1.51 |

**MR-GR overlapping target genes**

| GO term(s) | Category | Enrichment score |
|---|---|---|
| **Cytoskeleton, microtubule** | CC | 1.79 |
| **Synapse** | CC | 1.76 |
| **Positive regulation of protein binding** | BP | 1.52 |
| **Membrane/insoluble fraction** | CC | 1.49 |
| **Ion binding** | MF | 1.41 |
| **Regulation of synaptic plasticity/transmission** | BP | 1.40 |

**GR-exclusive target genes**

| GO term(s) | Category | Enrichment score |
|---|---|---|
| **Cell/neuron projection, dendrite** | CC | 6.48 |
| **Enzyme/kinase binding** | MF | 3.30 |
| **Membrane/insoluble fraction** | CC | 3.26 |
| **Cell adhesion** | BP | 2.87 |
| **Apoptosis** | BP | 2.52 |
| **Response to endogenous/hormone stimulus** | BP | 2.39 |
| **Response to oxidative stress** | BP | 2.30 |
| **Synaptic vesicle** | CC | 2.19 |
| **Cytoskeleton organization** | BP | 1.78 |
| **Immunoglobulin** | CC | 1.76 |